Received: 8 September 2017 | Revised: 28 November 2017 | Accepted: 5 December 2017

DOI: 10.1002/cmr.a.21415

RESEARCH ARTICLE

WILEY

Evolutionary algorithms and nuclear magnetic resonance of oriented molecules

E. Elliott Burnell[1] | **Cornelis A. de Lange**[2] | **Ronald Y. Dong**[3] | **W. Leo Meerts**[4] | **Adrian C. J. Weber**[5]

[1]Chemistry Department, University of British Columbia, Vancouver, BC, Canada

[2]Laser Centre, Vrije Universiteit, Amsterdam, The Netherlands

[3]Department of Physics and Astronomy, University of British Columbia, Vancouver, BC, Canada

[4]Felix Laboratory, Molecular- and Biophysics Group, Institute for Molecules and Materials, Radboud University, Nijmegen, The Netherlands

[5]Department of Chemistry, The University of Winnipeg, Winnipeg, MB, Canada

Correspondence
E. Elliott Burnell, Chemistry Department, University of British Columbia, Vancouver, BC, Canada.
Email: elliott.burnell@ubc.ca

This article is a contribution to the special issue in honor of Alex Bain.

Funding information
Harrison Trust (UBC)

Abstract

In this article, we discuss the progress achieved with the use of evolutionary algorithms for the analysis of ^{1}H Nuclear Magnetic Resonance spectra of solutes in orientationally ordered liquids. With these tools the analysis of extremely complex spectra that were hitherto impossible to solve has now become eminently feasible. We discuss applications to 2 molecules of special interest: (a) hexamethylbenzene, which is a text book example of steric hindrance between adjacent rotating methyl groups; and (b) cyclohexane which is the standard example of interconversion between various molecular conformations. New interesting physics is obtained in both cases.

KEYWORDS

cyclohexane, evolutionary algorithms, hexamethyl benzene, liquid crystal, orientational order

1 | INTRODUCTION

Nuclear Magnetic Resonance (NMR) of molecules orientationally ordered in liquid-crystal solvents generally shows spectra that look very different from those observed in isotropic solvents. The second-rank tensor that describes the direct dipolar coupling between every pair of magnetic dipoles is traceless and thus not observed in an isotropic environment. Hence, spectra in isotropic solvents are relatively simple. In contrast, in a liquid-crystal environment direct dipolar interactions are no longer averaged to zero. In solvents that show a degree of orientational order, these dipolar couplings survive, and generally completely dominate the solute NMR spectra. Since the magnitudes of dipolar couplings depend on $\frac{1}{r_{ij}^3}$ (where r_{ij} is the distance between magnetic nuclei i and j), NMR spectra of such solutes contain valuable information about their geometrical structure. This is true not only for '*rigid*' solutes that occur in a single conformation in which the internal motions are described by the vibrational normal modes, but also for solutes that can occur in several conformations between which interconversion may take place. In the latter case the direct dipolar couplings contain information about the interconversion process.[1-7]

In addition to the direct dipolar couplings that are observed in solutes that show some degree of orientational order, also tensor elements or combinations thereof of the indirect couplings, chemical shielding tensors and

quadrupolar couplings are not averaged to zero and hence affect the NMR spectrum.[1-7] In the present paper, we shall focus on the ^{1}H NMR spectra of the solutes hexamethylbenzene (HMB) and cyclohexane that are indeed completely dominated by dipolar couplings. Compared to the dominating role of the dipolar couplings, the other contributions to the ^{1}H NMR spectra tend to be minor.

Since dipolar couplings occur between every pair of magnetic nuclei, the complexity of the resulting NMR spectra increases spectacularly with the number of nuclei, in our case ^{1}H. As an example, we show in Figure 1 the NMR spectra of partially oriented members of a series of alkanes, starting with the relatively simple CH_4 (methane), C_2H_6 (ethane), C_3H_8 (propane), and the more complex C_4H_{10} (*n*-butane), C_5H_{12} (*n*-pentane), and C_6H_{14} (*n*-hexane). Even a superficial inspection of the NMR spectra of the longer alkanes shows their extreme complexity.[8-14]

Although the measurement of NMR spectra of solutes that show some degree of orientational order is an art in itself, it will be obvious that obtaining the various spectral parameters from highly complex spectra is not a simple task. Clearly, the topic of how to analyse such spectra (which show a very large number of transitions that may or may not be subject to extensive spectral overlap) is key to the applicability of the liquid-crystal NMR method.

The art of spectral analysis has a long history. For solutes that contain few magnetic nuclei, simple NMR spectra arise and they can be essentially analysed on inspection. The solutes H_2, HD, D_2, HT, DT, and T_2 are excellent examples.[6,15-17] For larger solutes it usually helps to exploit the symmetry of the molecule.[1,2] For solutes with little or no symmetry computer programmes such as LEQUOR,[18] a computer program based on LAOCOON,[19] were developed at an early stage. From a given set of spectral parameters the corresponding NMR spectrum can be calculated and then compared to what is obtained experimentally. If one is lucky, certain transitions can be recognized and assigned. Next, the parameters are adjusted employing least squares methods and in a step-wise manner more and more transitions are designated. Entire generations of PhD students often spent months on analysing a single spectrum in this labor-intensive manner. Still, if solute species contained more than about 8 spins, even this computer method fell short. In many laboratories unanalysed spectra were stored in despair awaiting better days.

With the advent of more powerful computer technology better days did indeed arrive. First, attempts were made to develop computer algorithms for automated spectral analysis. These methods, although meant to operate without operator interference, met with limited success and never quite fulfilled their promise. The number of spectra that have been analysed with such methods remains limited until today.[20-29] Also, in the spirit of the present paper, a few attempts to apply Genetic Algorithms (GAs) were made, but no further developments were reported.[30,31]

An approach that was pioneered by the present authors led to a robust and highly effective method of automated spectral analysis that by now can be operated in routine fashion. The method is based on sophisticated evolutionary algorithms (EAs) which were first developed as a mathematical way to describe genetics and evolution. The associated algorithms have proved to be eminently successful in the physical sciences. The first application was to optical spectra measured for chemical complexes in the gas phase to resolve their rotational structure.[32] Later these methods were modified and applied to the NMR spectra of partially oriented species dissolved in liquid-crystal solvents. In fact, this latter application is a more stringent test of EAs than is provided by the optical spectra, since the NMR spectra are devoid of any regularity that one can rely on. By now

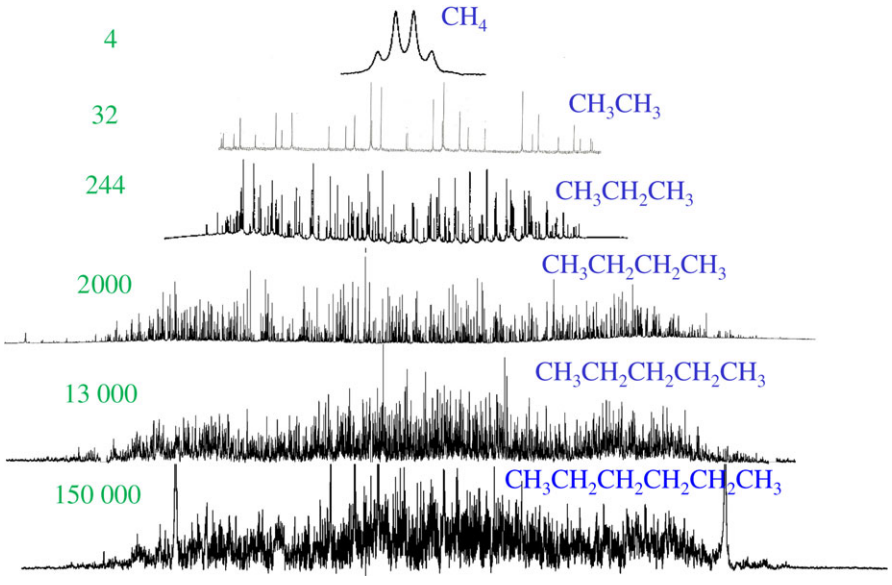

FIGURE 1 NMR spectra of solutes methane, ethane, propane, butane, pentane, and hexane orientationally ordered in nematic liquid crystal solvents. The number of transitions is indicated to the left of each spectrum

the application of EAs to NMR has proved to be extremely successful.[33] In a sense the holy grail of an analytical tool that can extract all the relevant parameters from highly complex spectra in a fully automated fashion is now there to be utilized in circumstances that only a few years ago were unthinkable. With the employment of sophisticated EAs the liquid-crystal NMR method has obtained a new lease of life.

In the present paper, we shall apply EAs to the extremely complex ^{1}H NMR spectra of $C_{12}H_{18}$ (hexamethylbenzene, HMB)[34] and C_6H_{12} (cyclohexane). In both solutes internal motion is important. In HMB the question arises whether the rotation of a single methyl group is hindered by that of adjoining ones. In cyclohexane the time scale for interconversion between various conformations can affect the NMR spectrum. For both molecules extreme spectral overlap is a key issue due to the large number of coupled protons. In this paper, we shall demonstrate how the application of EAs to highly complex NMR spectra provides an excellent tool for making important inroads into problems in chemical physics that hitherto were totally out of range.

2 | THEORY

When solutes are dissolved in liquid-crystal solvents that have cylindrically symmetric apolar phases, the molecular tumbling of the solute molecules is no longer isotropic. In addition to terms that occur in the isotropic high-resolution NMR Hamiltonian, a number of new anisotropic terms arise. In the limit of high magnetic field, the NMR Hamiltonian becomes:[3-5]

$$\begin{aligned}\hat{H} = &-\frac{B_Z}{2\pi}\sum_i \gamma_i\left(1-\sigma_i^{\mathrm{iso}}-\sigma_i^{\mathrm{aniso}}\right)\hat{I}_{i,Z}\\ &+\sum_{i<j} J_{ij}^{\mathrm{iso}}\hat{\mathbf{I}}_i\cdot\hat{\mathbf{I}}_j\\ &+\sum_{i<j}\left(2D_{ij}^{\mathrm{aniso}}+J_{ij}^{\mathrm{aniso}}\right)\left[\hat{I}_{i,Z}\hat{I}_{j,Z}-\frac{1}{4}\left(\hat{I}_{i,+}\hat{I}_{j,-}+\hat{I}_{i,-}\hat{I}_{j,+}\right)\right]\\ &+\sum_i \frac{q_i^{\mathrm{aniso}}}{4I_i(2I_i-1)}\left(3\hat{I}_{i,Z}^2-\hat{\mathbf{I}}_i^2\right).\end{aligned} \tag{1}$$

Here, $\sigma_i^{\mathrm{aniso}}$ is the anisotropic contribution to the chemical shielding of nucleus i, J_{ij}^{aniso} the anisotropic contribution to the indirect spin coupling between nuclei i and j, and D_{ij}^{aniso} the anisotropic direct dipolar spin coupling between nuclei i and j. The final term with q_i^{aniso} signifies the quadrupolar coupling contributions for nuclei i with spin $I \geq 1$. In the following, we shall focus on ^{1}H magnetic nuclei. Indirect couplings between 2 ^{1}H nuclei are to a very good approximation isotropic.

The solute undergoes internal motions that are due to small-amplitude vibrational normal modes and may also involve large-amplitude conformational change. Usually, the timescale for conformational change is much shorter than the timescale required for NMR motional averaging. Hence, NMR spectra are then observed that are an average over all conformations. In particular, the observed dipolar couplings can then be expressed as:[6,7,35]

$$D_{ij} = \sum_n p^n \sum_{k,l} d_{kl,ij}^n S_{kl}^n, \tag{2}$$

where we drop the superscript aniso, where p^n is the probability of conformation n, and $d_{kl,ij}^n$ is given by:

$$d_{kl,ij}^n = -\frac{h\gamma_i\gamma_j}{4\pi^2}\left(\cos\theta_{ij,k}^n \cos\theta_{ij,l}^n / r_{n,ij}^3\right), \tag{3}$$

with $\cos\theta_{ij,k}^n$ the cosine of the angle between the ij direction in the molecule in conformation n, and k and l conformer-fixed axes.

When interconversion is not much faster than the NMR motional averaging time scale, line broadening may be observed that represents the signature of the interconversion process. We shall come back to this point in the context of our discussion on cyclohexane.

The Saupe order parameters for each conformation n are given by

$$S_{kl}^n = <\frac{3}{2}\cos\theta_{k,Z}^n \cos\theta_{l,Z}^n - \frac{1}{2}\delta_{kl}> \tag{4}$$

where $\cos\theta_{k,Z}^n$ is the cosine of the angle between the molecular k direction in conformation n and the space-fixed Z direction of the external magnetic field B_Z. The angular brackets indicate an average over all internal motions of the conformer n. There is a maximum of 5 independent order parameters for every conformation, and molecular symmetry can reduce this number.

Note that the observed dipolar couplings are always averages over both small- and large-amplitude internal motions. Because correcting for these internal motions requires additional information that is not always available, for instance about molecular force fields, such motions limit the accuracy with which geometrical information can be obtained from liquid-crystal NMR.[36]

3 | EXPERIMENTAL

Both hexamethylbenzene (HMB) and cyclohexane were studied as solutes in the nematic liquid crystal Merck ZLI-1132 (1132 for short), a nematic phase composed of 24% *trans*-4-*n*-propyl-(4-cyanophenyl)-cyclohexane, 36% *trans*-4-*n*-pentyl-(4-cyanophenyl)-cyclohexane, 25% *trans*-4-*n*-heptyl-(4-cyanophenyl)-cyclohexane, and 15% *trans*-4-*n*-pentyl-(4-cyanobiphenyl-4)-cyclohexane. HMB was obtained

from Aldrich (Milwaukee, WI, USA). A sample of approximately 10 mol per cent was made up in 1132 and a small quantity of 1,3,5-trichlorobenzene (tcb) was added as an orientational reference. The sample tube was placed into a Bruker 400 MHz Inverse spectrometer magnet at room temperature (298 K). ^{1}H NMR spectra were accumulated by adding 1742 scans. A spectral width of about 14 kHz was measured and line widths of typically 6 Hz were obtained.

A sample of approximately 6.8 mol per cent cyclohexane was made up in 1132 and again some tcb (0.2 mol per cent) was added as an orientational reference. ^{1}H spectra were obtained by adding 256 scans for a range of temperatures at 5K intervals (see Figure 2). A spectral width of about 8 kHz was measured and solute line widths varied strongly as a function of temperature, indicating interconversion dynamics.

The computer calculations used to fit the experimental spectra using evolutionary algorithms were carried out on a standard cluster. The wall clock time for cyclohexane was 4 h using 24 processors in parallel. For HMB this was 2 h using 20 processors.

4 | THEORY OF EVOLUTIONARY ALGORITHMS FOR THE ASSIGNMENT AND FIT OF SPECTRA

Increasing resolution and/or sensitivity of spectroscopic methods leads to increasing complexity of the spectra. This complexity stands in the way of extracting the spectroscopic parameters that describe the spectrum (see for example the spectra of cyclohexane at different temperatures in Figure 2). In the present paper we describe novel strategies to deal with this problem. Analysing complex spectra has a long history. The classical evaluation of the parameters that are needed to describe high-resolution spectra was based for decades on pattern recognition by eye, i.e. relied on the experience of the user.

In the past decades computational tools have been developed that are able to handle complex multi-parameter optimizations intelligently and within an acceptable time interval. The use of Evolutionary Algorithms (EAs) for solving such highly nonlinear and complex processes in science and engineering has become widespread. Although they are conceptually simple, their ability in avoiding local optima and instead finding the global optimum is remarkable and makes them suitable to handle complex optimization problems.

Evolutionary Algorithms represent a set of general purpose probabilistic search methods based on natural evolution. These algorithms mimic the concepts of natural reproduction and selection processes. The basic idea in EAs is to create an artificial environment which encodes the search problem into biology-like terms.

From a spectroscopic point of view, the EA approach reproduces this behavior to fit an experimental spectrum with a model based upon the differences in the eigenvalues of the Hamiltonian such as $\hat{H}$ given by Equation (1).

Three main different EAs have been developed over the years: The genetic algorithm (GA) by Holland,[37] the Evolutionary Strategy (ES) by Rechenberg,[38] and the Evolutionary Programming by Schwevel.[39]

For the automatic assignment and analysis of the high-resolution NMR spectra we have initially used the Genetic Algorithm (GA).[32] However, lately we mainly used an Evolution Strategy (ES) in our procedures, in particular the Covariance Matrix Adaptation Evolution Strategy (CMA-ES).[40]

4.1 | The genetic algorithm

A detailed description of the GA used in the automatic assignment and fitting of the spectra described in this paper can be found in ref. 32.

Each of the molecular parameters in $\hat{H}$ can be thought of as a gene encoded in binary or real type. The vector of all genes, which contains all molecular parameters, is called a chromosome. In an initial step the values of all parameters are set to random values between lower and upper limits which are chosen by the user. The quality of the solutions then are evaluated by a fitness function.

One optimization cycle, including evaluation of the fitness of all solutions, is called a generation. Pairs of chromosomes are selected for reproduction and their information is combined via a crossover process. Since crossover combines information from the parent generations, it basically explores the fitness landscape. The value of a small number of spectral parameters is changed randomly by a mutation operator. Mutation can be viewed as exploration of the fitness surface. The best solutions within a generation are excluded from mutation. This elitism prevents already good solutions from being degraded. Mutation prevents the calculation from being trapped in local minima, as is often the case with more conventional fitting routines. A flow-chart of the procedure is shown in Figure 3.

4.2 | The evolution strategy

The evolution strategy algorithm starts with 1 or more parent(s). A parent is a trial solution that corresponds to a set of parameters like in the genetic algorithm. From this parent an offspring of multiple children is generated. The quality or performance of these children is checked and depending on the strategy the next parent is generated.

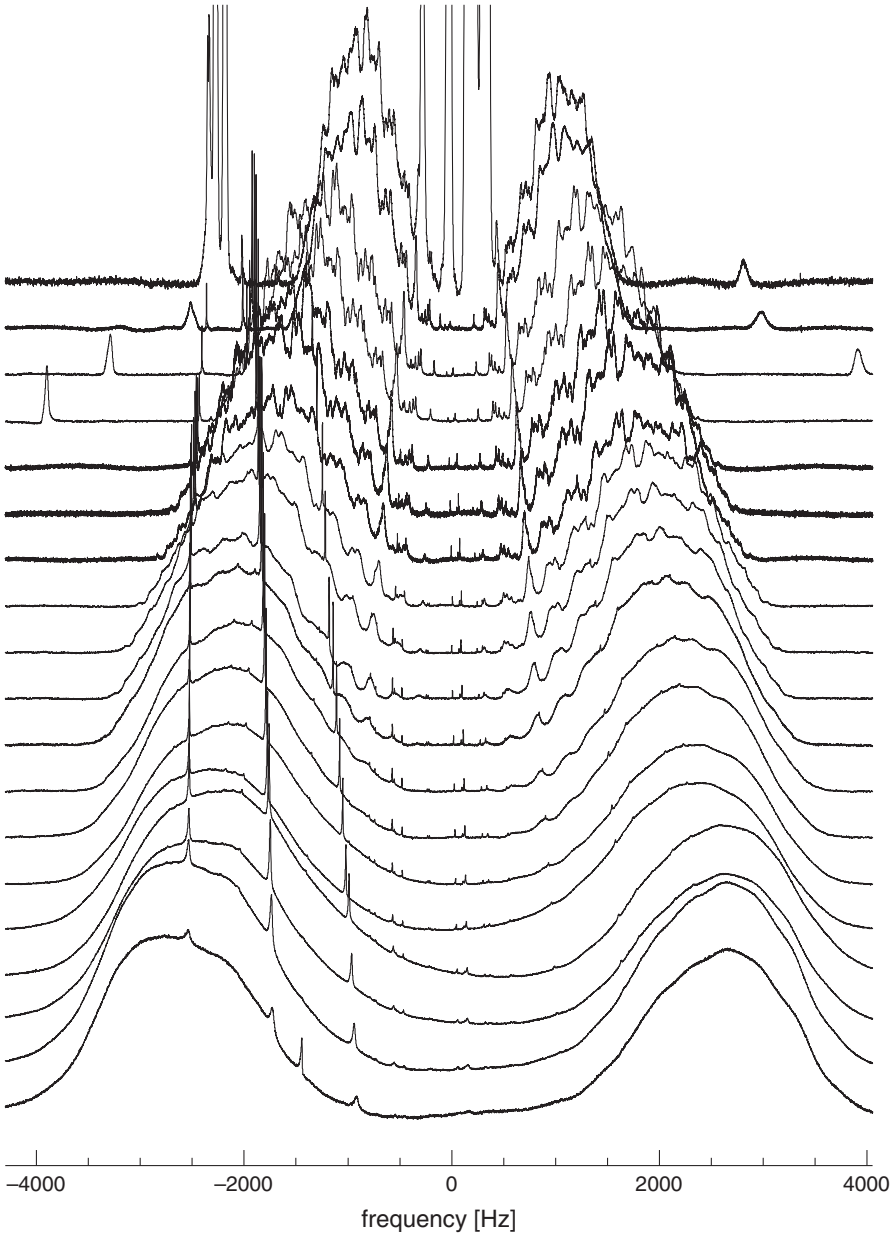

FIGURE 2 NMR spectra of cyclohexane orientationally ordered in the nematic liquid crystal 1132. The top spectrum at 332.4 K is from the 2-phase region of solute and solvent in a mix of nematic and isotropic phases. The next spectrum down is at 331.3 K, and temperature decreases by 5.7 K for each lower spectrum. The 1:2:1 triplet of sharp lines from the 1,3,5-trichlorobenzene (added as an orientational reference, and also to provide an estimate of rigid solute line width) is seen in each spectrum

There are several different strategies for the generation of the offspring as well as the generation of the next parent. For a more detailed description see ref. 38.

The offspring is created from the parent(s) in a mutative step-size control. A drawback of the standard ES is the fact that the mutations of the decision and the strategy parameters are subject to independent random processes. If for example an individual with a large step size undergoes only a very small change in the decision parameters and this small change turns out to yield a high fitness, the large step size will be inherited to the next generation. As a result the fitness in the next mutations may worsen. This problem is resolved in derandomized (DR) algorithms which make the random mutations in decision and strategy parameters dependent on each other. This idea was implemented initially as DR1 and soon improved by the concept of accumulated information,[41] which will be called DR2. In DR2 the history of the optimization is recorded and the evolution of the mutation ellipsoid is partially governed by past successful mutations.

A further improvement was achieved by Hansen and Ostenmeier[40] with the Covariance Matrix Adaptation Evolution Strategy (CMA-ES). It turns out to be a particularly reliable and highly competitive evolutionary algorithm for local optimization and, surprisingly at first sight, also for global optimization.[42] The CMA-ES does not leave the choice of strategy parameters open to the user — only the population size can be set. Finding good strategy parameters is considered to be part of the algorithm design.

Figure 4 depicts the first 4 generations of an evolutionary strategy and demonstrates the effect of the chosen

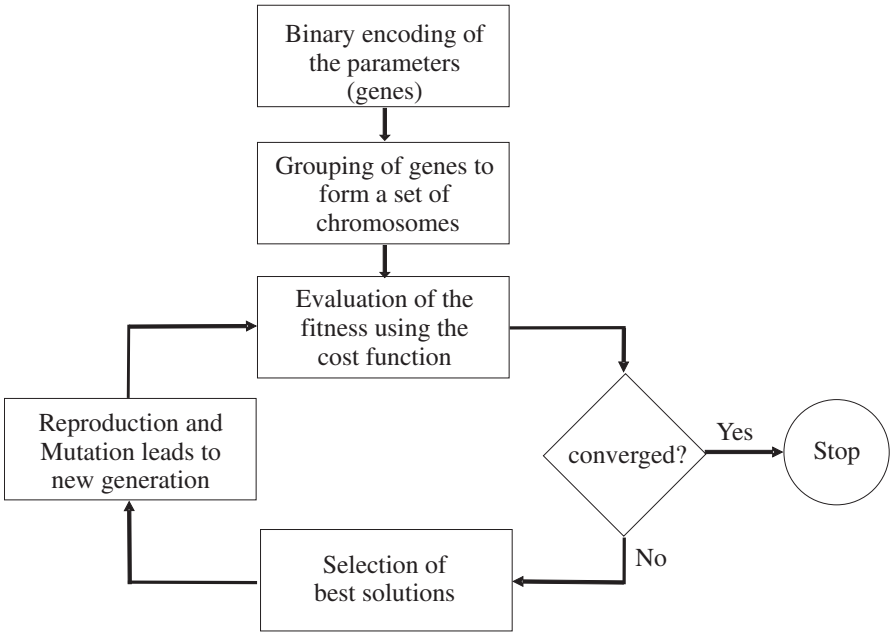

FIGURE 3 Schematics of the GA-process. Reproduced with permission from ref [33].

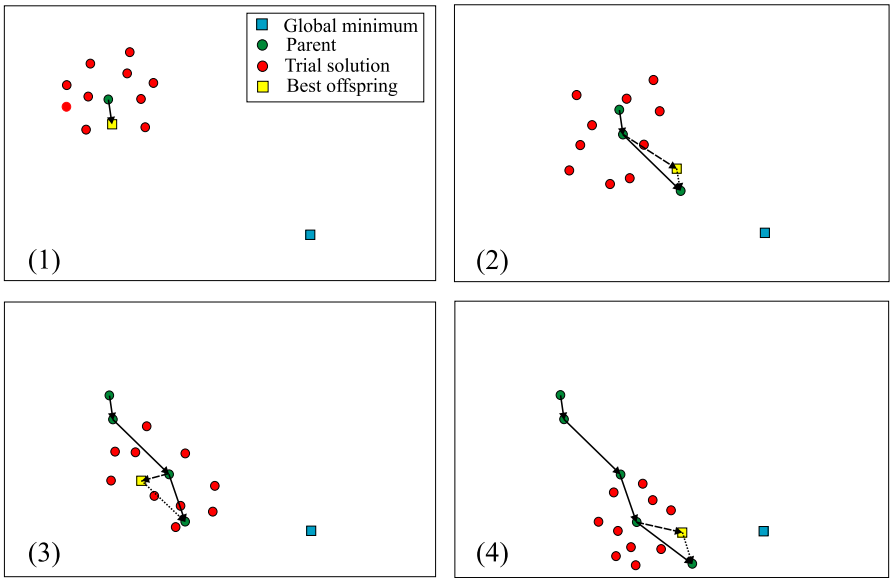

FIGURE 4 The first 4 generations of an Evolution Strategy: (1) An initial population is generated, and the best offspring is used as the next parent. (2) The offspring is spread over a larger area in the second generation due to the relatively large step made in the previous generation. The vector from the parent to the best offspring (dashed line) is combined with the (shortened) mutation vector of the last generation (dotted line) to generate the new parent (solid line). (3) Due to the correlation between the past 2 mutations the search range has been extended again in the general direction of both mutations while it has been limited in the perpendicular direction. The best offspring is now a local minimum. The memory effect of the evolutionary algorithm, which incorporates past mutation vectors into the calculation of the next parent, helps to overcome the local minimum and the next parent is still closer to the global minimum. (4) The barrier between the local and global minima has been overcome, and the optimization is progressing towards the global minimum. Reproduced with permission from ref [33]

strategy. In general the Evolution Strategies converge faster and are more robust than the genetic algorithm.

4.3 | The fitness function for the analysis of spectra

A proper choice of the fitness function is of vital importance for the success of the EA convergence. It should be calculated sufficiently fast and give a quantitative measure of the goodness of a fit. The value of the fitness function is used to select potential solutions that will survive the current generation, and those that will die out.

Frequently, the deviation of a solution from an objective function is measured via least squares. While for many optimization problems least squares are a reasonable choice, they fail for an evaluation of the agreement of 2

spectra in the course of the fit. Other objective functions that have been tested for optimization processes are the Manhattan distance as simple absolute distances of the solution from the aim function,[43] Garuti's compatibility index,[44] which is based on the inner product between vectors, Saaty's compatibility metric,[45] or Pearson correlation coefficient.[46]

Meerts et al[47] have defined a proper fitness function F_{fg} for the use in EA as:

$$F_{fg} = \frac{(\boldsymbol{f},\boldsymbol{g})}{\|\boldsymbol{f}\|\|\boldsymbol{g}\|} \tag{5}$$

Here, $\boldsymbol{f}$ and $\boldsymbol{g}$ are the vector representations of the experimental and calculated spectrum, respectively. The inner product $(\boldsymbol{f}, \boldsymbol{g})$ is defined with the metric $\boldsymbol{W}$ which has the matrix elements $W_{ij} = w\ (|j\text{-}i|) = w(r)$ as:

$$(\boldsymbol{f},\boldsymbol{g}) = \boldsymbol{f}^{\boldsymbol{T}}\boldsymbol{W}\boldsymbol{g}, \tag{6}$$

and the norm of $\boldsymbol{f}$ as $\|\boldsymbol{f}\| = \sqrt{(\boldsymbol{f},\boldsymbol{f})}$; similar for $\boldsymbol{g}$. For $w(r)$ a triangle function was used[48] with a width of the base of Δw:

$$w(r) = \begin{cases} 1 - |r|/(\frac{1}{2}\Delta w) & \text{for} \quad |r| < \frac{1}{2}\Delta w \\ 0 & \text{otherwise.} \end{cases} \tag{7}$$

The use of a broadening function $w(r)$ results in a smoother error-landscape which allows an easier optimization, since narrow valleys on the fitness surface are broadened, allowing the algorithm to converge more smoothly to the correct values. It should be mentioned that the use of the broadening function improves the performance of the GA greatly, but is not needed for the convergence of the CMA-ES.

5 | AUTOMATIC BASELINE REMOVAL IN NMR SPECTRA

Slow baseline variations due to unresolved solvent contributions in NMR spectra of solutes in liquid-crystal solvents are a well-known problem. For sparse spectra manual removal of the background is quite feasible. A non-flat baseline due to (broad) NMR signals arising from the solvent and experimental imperfections becomes more pronounced for weak NMR spectra. Furthermore, if the number of lines further increases such that overlap of transitions occurs, a manual removal is no longer possible. The combination of the above mentioned problems gave rise to the need to automatically remove the background from both the solvent as well as from overlapping lines. This is achieved by removal of a smoothened spectrum from both the experimental and calculated spectra.

The smoothed experimental spectrum $\boldsymbol{f^S} = (f_1^S, f_2^S, .. f_N^S)^T$ is defined as:

$$f_i^S = \frac{1}{n_s + 1} \sum_{j=i-n_s/2}^{i+n_s/2} f_j \tag{8}$$

Here, n_s is the number of points over which the smoothening should be performed. The smoothening over the calculated spectrum $\boldsymbol{g}$ is carried out identically, resulting in $\boldsymbol{g^S} = (\boldsymbol{g_1^S}, \boldsymbol{g_2^S}, .. \boldsymbol{g_N^S})^{\boldsymbol{T}}$:

$$g_i^S = \frac{1}{n_s + 1} \sum_{j=i-n_s/2}^{i+n_s/2} g_j \tag{9}$$

The actual spectrum which is fitted is $\boldsymbol{f^R} = \boldsymbol{f} - \boldsymbol{f^S}$ against $\boldsymbol{g^R} = \boldsymbol{g} - \boldsymbol{g^S}$, i.e. in Equation (5) $\boldsymbol{f}$ and $\boldsymbol{g}$ are replaced by $\boldsymbol{f}^R$ and $\boldsymbol{g}^R$, respectively.

The idea behind this method is that removal of a smoothened spectrum removes the baseline of experimental source not present in the calculated spectrum. At the same time features in the spectrum which are on top of a background caused by overlapping transitions become more pronounced. So in the global fit the local features contribute more effectively in the fitness. This increases the dynamics of the fitness function. The effect of the automatic background removal is demonstrated in Figure 5 for the case of hexamethylbenzene.

6 | RESULTS AND DISCUSSION

6.1 | Hexamethylbenzene

Hexamethylbenzene (HMB, Figure 6) is an interesting molecule not only because of its aesthetically pleasing appearance. The presence of 6 methyl groups, each of which undergoes rotational motion, raises questions about steric hindrance. Do the 6 methyl groups undergo their rotational motions completely independent of each other, or are their rotations correlated in some way or another? In the case of correlated motion, 2 possible modes can be envisaged. First, all methyl groups rotate in the same direction (for example, all α_i increase), a process we call co-rotating or anti-gearing. Second, the methyls act as cog-wheels with adjacent methyl groups rotating in opposite directions (for example α_i and α_{i+1} change by equal but opposite amounts), a mode we call counter-rotating or gearing. In the latter case the 6 methyl groups together form a hexagonal gear, which is an interesting concept physically.

Assuming a planar geometry for HMB and independent rotation of all methyl groups across a sixfold barrier, thus neglecting interactions between them, the molecule possesses a sixfold symmetry axis, z. Hence, its partial orientational order is determined by a single independent Saupe

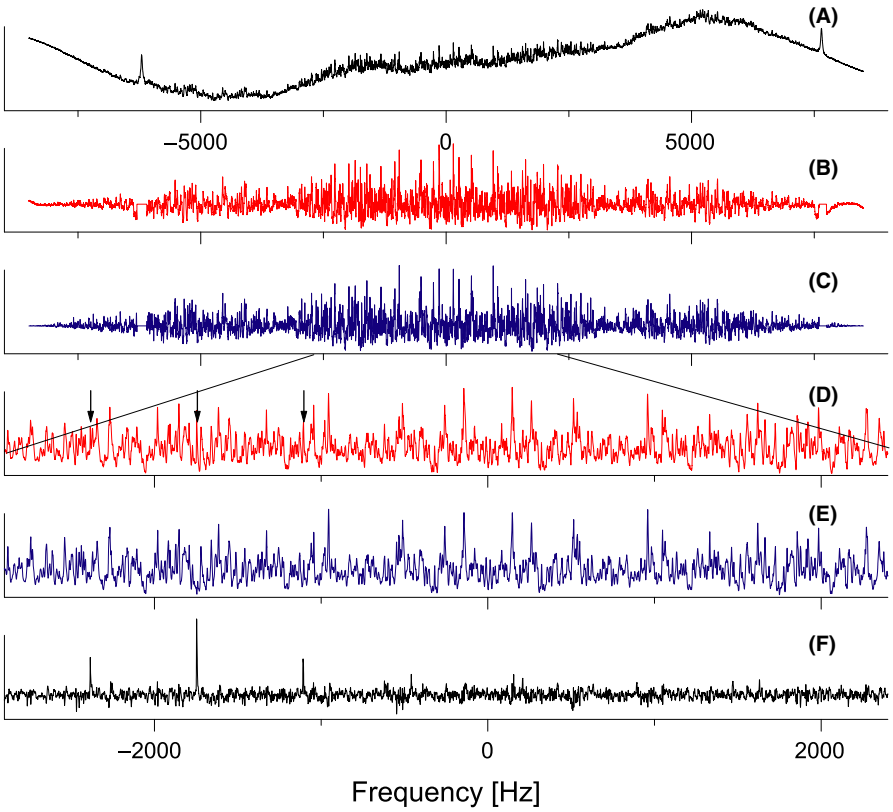

FIGURE 5 A demonstration of the automatic baseline removal. Experimental and fitted NMR spectra of hexamethylbenzene in 1132 at 298 K.[34] A, Experimental spectrum (1742 scans). The line broadening applied before Fourier transform is 0.1 Hz. The experimental line full width at half height is of order 6 Hz. The program LEQUOR[18] was used to calculate the simulated NMR spectra. In order to deal with the broad underlying liquid-crystal NMR signal in the experimental spectrum and to improve the dynamics in the spectra, a background signal averaged over 274 Hz is subtracted from both the experimental and calculated spectra depicted in B through E.[33] Here B and D are the full and zoomed in experimental spectra, while C and E are the corresponding calculated ones. The blowups D and E show the excellent fit obtained. The arrows in D point to the lines of the solute tcb triplet. The high quality of the fit is demonstrated in F, the difference between D and E. The tcb lines stand out from the noisy background left after the subtraction. The tcb transitions are spaced $3D_{tcb}$ apart giving $D_{tcb} = -212.9 \pm 0.4$ Hz. The HMB couplings obtained from the fit are $D_{1,2} = 1629.4 \pm 0.4$ Hz, $D_{1,4} = -456.6 \pm 0.2$ Hz, $D_{1,7} = -89.4 \pm 0.3$ Hz and $D_{1,10} = -57.1 \pm 0.4$ Hz. Modified from Figure 3 of ref [34], reproduced with permission

orientation parameter S_{zz}. The entire spectrum scales effectively with this order parameter. Despite that the solute contains as many as 18 protons and shows more than 350 000 transitions (with intensity >1% that of the strongest one), this feature is very helpful in the analysis.

The spectrum of HMB is presented in Figure 5. Spectral analysis was performed using CMA-ES with automatic baseline removal (see section 5). The agreement between experimental and fitted spectra is generally excellent, and the earlier hard labor of analysing experimental spectra such as those reported here has been reduced to virtually a routine activity. This represents the true power of the EA. The liquid crystal 1132 in addition gives rise to 2 strong, broad peaks. These peaks were artificially removed before starting the EA fitting procedure.

The NMR spectral analysis algorithm LEQUOR[18] is a key ingredient of our EA fitting approach. With 18 protons there are $2^{18} = 262\ 144$ proton spin energy levels with the largest Hamiltonian matrix to be diagonalized 48 620 × 48 620. With the composite spin approach, with each methyl group treated as spin $I = \frac{3}{2}$ or $\frac{1}{2}$, the largest matrix (for all methyl groups of spin $I = \frac{3}{2}$) reduces to 580 × 580, thus considerably alleviating the computational effort.

Hexamethylbenzene has been the subject of ab initio calculations.[49,50] In these calculations several configurations of the 6 methyl groups are considered (some examples are in Figure 7). Accurate direct dipolar couplings averaged over the intramolecular methyl rotations are derived from our EA fitting procedure. Especially the *ortho* intermethyl coupling is interesting because it is quite sensitive to rotational details of adjacent methyl groups. From our results it can be concluded that, in agreement with the ab initio results, the 6 methyl groups show significantly hindered anti-geared rotations, while geared rotation with adjacent methyl groups moving in a counter-rotating

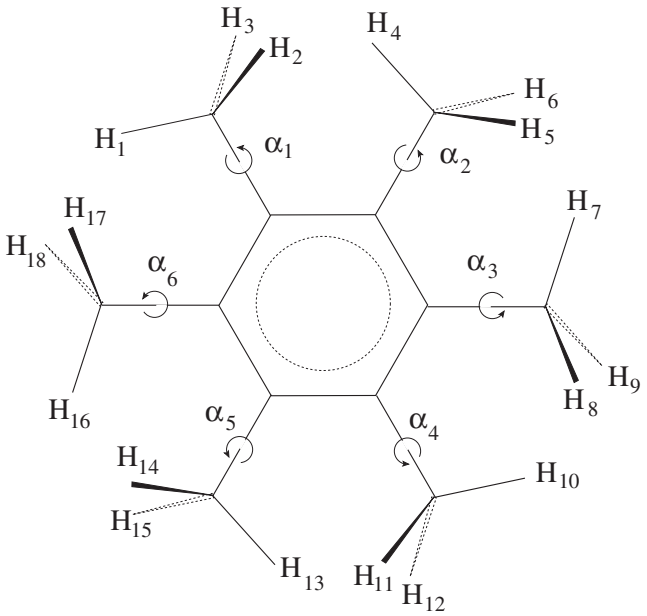

FIGURE 6 Hexamethylbenzene. The angles α_i define the methyl rotation and are shown as zero. Reproduced with permission from ref [34]

fashion is favorable. Our experimental results therefore shed new light on an old problem. For a full account of this work we refer to the literature ref [34].

6.2 | Cyclohexane

Cyclohexane (Figure 8; see Figure 2 for ^{1}H NMR spectra of cyclohexane orientationally ordered in the nematic liquid crystal 1132 as a function of temperature) is the classic example of conformational interconversion studied by organic chemists. The predominant conformational change is from one chair to the other chair conformation. This change involves going through boat and twist boat intermediates. The boat and twist boat intermediates are much higher energy than the chairs, and thus their populations are very small and hardly contribute to the averaged NMR spectrum.

At sufficiently low temperatures (associated with slow interconversion, i.e. lower than the lowest T of Figure 2) one expects to observe an NMR spectrum from a single chair conformation that is governed by ten independent dipolar couplings. The spectrum should then broaden in the

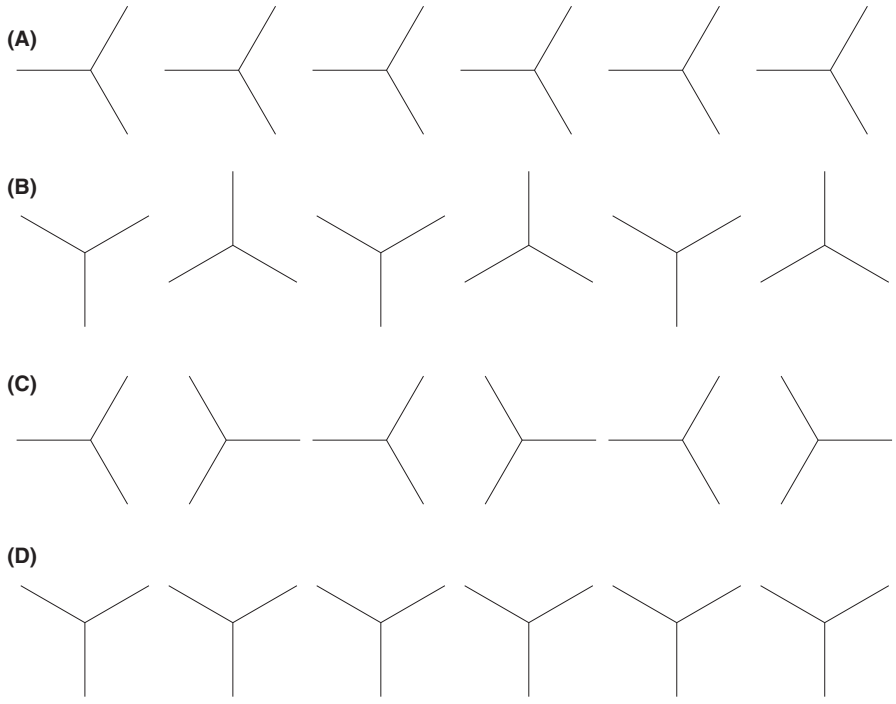

FIGURE 7 Interesting configurations of hexamethylbenzene. A, One of the low-energy configurations, having C_{6h} symmetry. B, A second low-energy configuration, having D_{3d} symmetry. C, One of the high-energy configurations obtained by rotating all methyls in B by −30 degrees. D, Another high-energy configuration, obtained by rotating all methyls in A by 30 degrees. A typical path for anti-gearing rotation of all methyl groups would take low-energy A (or B) to high-energy D (or C). A typical path for gearing rotation would take low-energy A to low-energy B and would avoid the high-energy C and D configurations. The barrier to geared rotation involves the small energy difference between configurations A and B. The potential to anti-geared rotation involves the difference in energy between the A and D (or B and C) configurations. Analysis of the NMR gives a large value for this barrier to anti-geared rotation (12.2 kcal/mol). Reproduced with permission from ref [34]: in that paper, it should state that Figure 2C is obtained by rotating all methyls in B by −30 degrees, and Figure 2D is obtained by rotating all methyls in A by 30 degrees

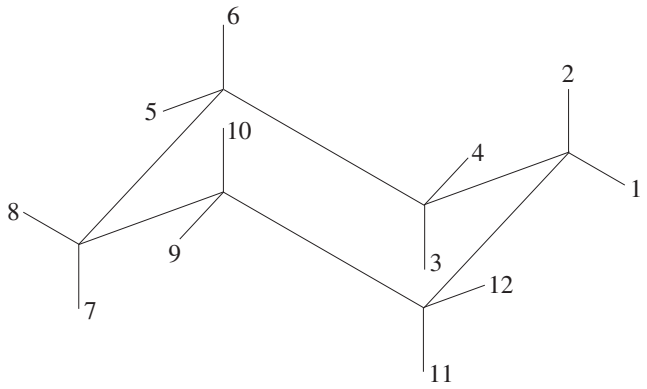

FIGURE 8 Cyclohexane in a chair conformation

intermediate exchange limit (lower temperatures in Figure 2), with a dearth of sharp features. As temperature rises, the rate of chair-chair interconversion increases until an averaged spectrum is observed (upper plots in Figure 2). These averaged spectra are based on 7 $D_{i,j}$: the values of $D_{1,2}$, $D_{1,3} = D_{2,4}$, $D_{1,6} = D_{2,5}$, $D_{1,7} = D_{2,8}$, and the mean values of coupling pairs $D_{1,4}$ & $D_{2,3}$, $D_{1,5}$ & $D_{2,6}$, and $D_{1,8}$ & $D_{2,7}$.

In fitting the observed spectra we encounter a serious difficulty. We can try to fit the ^{1}H NMR spectra for a chair conformation that does not interconvert, which requires 10 different dipolar couplings, or we can assume the solute to be in the limit of fast interconversion, which would require 7 different dipolar couplings. When we start the fitting procedure with 10 or 7 dipolar couplings, in both cases convergence is obtained. When we start from 10 dipolar couplings, the fitting procedure partly but not completely removes the differences between axial-axial and equatorial-equatorial proton couplings. Further analysis shows that there is a large correlation between the values: the sums of these pairs of dipolar couplings that are averaged by the exchange are well fitted but the differences have a large error and are essentially zero within this error. Hence for our analysis we shall set the differences to zero (i.e. assume rapid exchange) and fit to 7 independent dipolar couplings. An example of the spectrum fitted with 7 different dipolar couplings is in Figure 9.

The 7 independent D_{ij} obtainable from the motionally averaged chair cyclohexane spectra measured at higher temperature can be used to extract geometrical information. We assume that the chair conformer dominates the NMR and that there is rapid exchange between the 2 chair forms. We also neglect other effects of non-rigidity in the cyclohexane. Then the proton molecular geometry is defined by

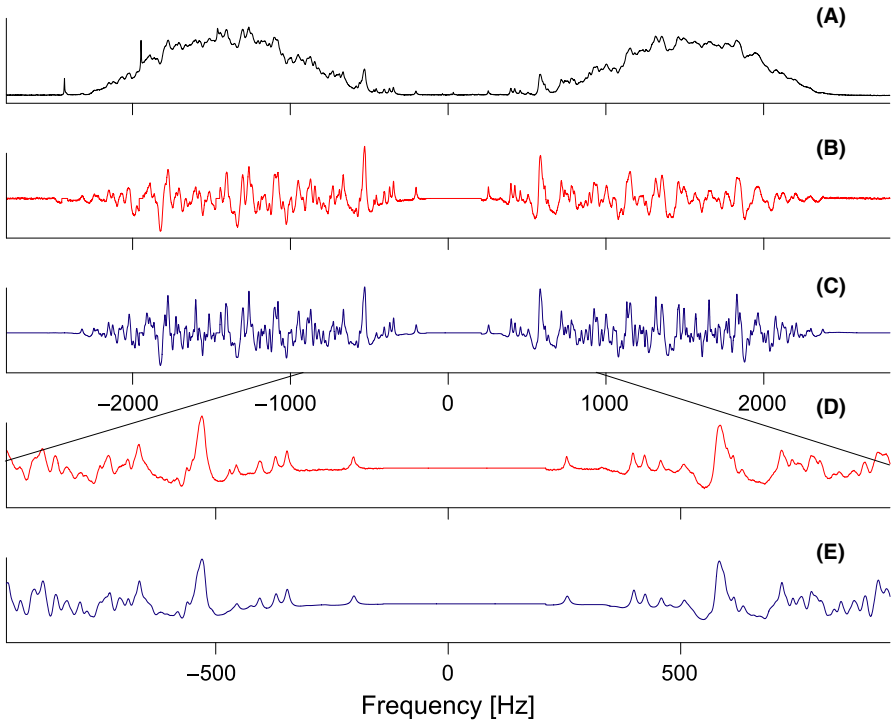

FIGURE 9 Experimental and fitted NMR spectra of cyclohexane in 1132 at 320 K. A, Experimental spectrum (256 scans). The program LEQUOR[18] was used to calculate the simulated NMR spectra. In order to deal with the broad underlying liquid-crystal NMR signal in the experimental spectrum and to improve the dynamics in the spectra, a background signal averaged over 109 Hz is subtracted from both the experimental and calculated spectra depicted in B through E. Here, B and D are the full and zoomed in experimental spectra, while C and E are the corresponding calculated ones. The blowups D and E show the excellent fit obtained. The experimental line full width at half height is of order 12 Hz, as seen for the ten non-overlapping transitions in the centre of the spectrum

TABLE 1 Proton coordinates in Å obtained from a fit to the dipolar couplings measured at 320 K. The NMR order parameter is $S_{zz} = -0.08278 \pm 0.00006$

Coordinate	From NMR	From G09
$y(1)$	2.498 ± 0.005	2.504
$y(2)$	1.507	1.507
$z(1)$	−0.150 ± 0.008	−0.127
$z(2)$	1.337 ± 0.007	1.342

The ratios of internuclear distances r_{ij}(NMR)/r_{ij}(G09) are 1.00674 for protons 1 and 2, 0.99675 for protons 1 and 7, and 0.99833 for protons 1 and 8.

4 unknown distances: the y and z coordinates of one axial and of one equitorial proton (the z axis is the C_3 symmetry axis and we choose the protons that lie in the symmetry plane with $x = 0$). Coordinates of the remaining protons are then obtained by symmetry, and the origin is fixed to the molecular centre. We use GAUSSIAN 09 MP2/aug-cc-pvdz[51] (G09 for short) to calculate the gas-phase proton molecular geometry of chair cyclohexane (Table 1). Møller-Plesset[52] second-order (MP2) perturbation theory was employed using Dunning's cc-pvdz basis set.[53]

Since the measured NMR D_{ij} involve products $\frac{1}{r_{ij}^3} S_{zz}$, 1 geometric coordinate needs to be fixed to provide the scaling for the molecular dimensions: we use the value of $y(2)$ from the G09 calculation for this purpose. The fit of 3 unknown coordinates and the order parameter S_{zz} to the NMR D_{ij} yields the results listed in Table 1. This table allows us to compare the NMR proton geometry with the G09 structure. The $y(1)$ and $z(2)$ coordinates agree within the NMR error while the $z(1)$ coordinates are within 0.023 Å. The NMR/Gaussian ratios of internuclear distances are given in the footnote to the table, and the excellent agreement, which justifies our various assumptions, can be taken as strong evidence of the nonimportance of other than the rapidly exchanging chair conformers.

If the populations of the boat and twist boat configurations were sufficiently large, then the NMR spectrum should give ratios of dipolar couplings that change with temperature (in the fast exchange limit) as the populations of boat conformations give significant contribution to the spectrum and hence the ratios. As the ratios do not change significantly with temperature we are unable to extract information about the boat and twist boat conformations.

Here, we are interested in using the higher-temperature spectra of Figure 2 to obtain information on the rate of chair-chair interconversion of orientationally ordered cyclohexane.

Analysis of the NMR spectrum in the intermediate exchange limit has been reported for simpler spin systems, for example cyclooctatetraene.[54] Such analysis is beyond the scope of this paper. However, examination of a much simpler system sheds light on the generalities of the problem. The classic example involves exchange of a proton between 2 sites with different chemical shifts.[1,55] The correlation time for the exchange is τ_c. For slow exchange 2 lines separated by $\Delta\nu$ are observed, 1 for each proton. As the exchange rate $1/\tau_c$ increases the peaks broaden and eventually coalesce into a single, broad line. With faster exchange, the broad line sharpens and has full width at half height (in Hz) $W_{\text{exch}} = M_2\tau_c/\pi$ where $M_2 = (\pi\Delta\nu)^2$ is the second moment (in per s^2) for the non-exchanging spectrum.

The liquid-crystal and solute orientational orders usually vary with temperature, and we can write the non-exchanging $\Delta\nu$ in terms of an order parameter S, i.e. $\Delta\nu = \Delta\nu_0 S$ where $\Delta\nu_0$ is the splitting in Hz for perfect alignment corresponding to $S = -0.5$. Then the non-exchange second moment M_2 will scale with S^2 and the exchange rate (in per s) becomes

$$\text{exchange rate} = 1/\tau_c = M_2^0 S^2/\pi W_{\text{exch}} \qquad (10)$$

where M_2^0 is the second moment for perfect alignment.

In the cyclohexane case the situation is much more complicated than discussed for the simple case above. Since during the chair-to-chair interconversion the axial-axial and equatorial-equatorial dipolar couplings exchange at a certain rate, the line broadening for each transition in the spectrum differs, depending on how much these dipolar couplings contribute to that transition. Hence, the line width of every transition is affected differently. With the huge number of transitions we have no other choice but to assume a line broadening that is identical for every transition and uniform across each spectrum. This is a serious but unavoidable limitation. The question is how to obtain sensible values for these uniform line widths as a function of temperature. We shall make the approximation that there is an effective, averaged M_2 for the (unknown) peak separations that scales as $M_2^0 S_{zz}^2$ with S_{zz} being the cyclohexane order parameter. If we have a value for M_2^0, we can then use Equation 10 to obtain a value for the exchange rate.

Estimation of the line width in the cyclohexane spectra which consist of almost completely overlapping lines is difficult. One possibility is to allow the line width to vary as a parameter in the EA fitting. This procedure does not yield satisfactory results. EA with overlapping lines tends to overestimate the line widths which then allows EA more flexibility in fitting the spectra.

An alternative approach and our method of choice utilizes the presence of 10 single-transition lines near the centre of the cyclohexane spectra and the 3 lines of the tcb (added as an internal orientational reference). If we assume that the line widths of rigid (non-exchanging) cyclohexane

and tcb are equal (a reasonable assumption as the molecules are roughly the same size and shape), then we obtain the exchange contribution (reported in Table 2) to the cyclohexane spectrum as $W_{exch} = W_{exp} - W_{tcb}$. These widths are readily measured at the higher temperatures. At lower temperatures, in addition to the problem of fitting a line width to the overall, broad spectrum, we may be entering the region where the central cyclohexane exchange line is no longer Lorentzian. Thus, we place no physical significance on the discrepancy between values obtained from the 10 sharp lines and those from an EA fit to the entire spectrum.

In order to use Equation 10 to obtain exchange rates from the line width and S_{zz} results in Table 2, we need a value for M_2^0. Here we obtain that value by fitting our results to get the best average agreement with the rate data from 2 earlier NMR studies, that of Pickett and Strauss[57] and that of Bain et al[58] The value obtained for $M_2^0 = 1.8 \times 10^7/s^2$ gives a $\Delta\nu \approx 110$ Hz, a value that compares favorably with the change in dipolar couplings upon exchange of roughly 50-300 Hz. This agreement shows that what we and others do is reasonable.

In Figure 10 we present an Arrhenius plot for our results, those of Pickett and Strauss and those of Bain et al for substituted cyclohexanes. We see that the temperature dependence of exchange rates is essentially the same for all 3 sets of results.

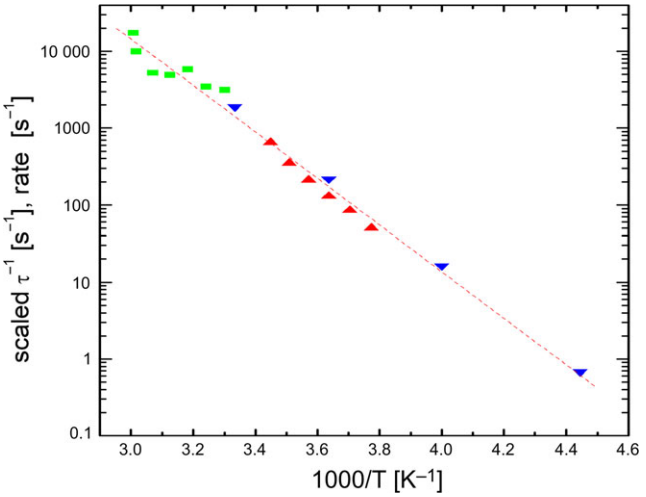

FIGURE 10 Chair-chair interconversion rate *vs* inverse temperature. A ln plot of the cyclohexane chair-chair exchange interconversion rate: down-triangles from Pickett et al[57] up-triangles from Bain et al[58]; closed squares from the present work obtained with line widths estimated visually from non-overlapping lines in the middle of the spectrum. To obtain rates, our inverse line widths are multiplied by the factor $S_{zz}^2 M_2^0/\pi$ with the fitting value of $M_2^0 = 1.8 \times 10^7/s^2$ to get the best average agreement between our results and the data of refs 57 and 58

7 | CONCLUSION

The use of evolutionary algorithms for the analysis of experimental ^{1}H NMR spectra of solutes in orientationally ordered liquids has led to enormous progress in the analysis of extremely complex spectra. In this paper it is illustrated how application of these algorithms makes spectral analysis of complex spectra such as those reported here an almost routine activity where without operator interference convergence is reached with a reasonable investment in computer power and time. To aid the reader, the developments that have taken place and have led to various novel evolutionary strategies are discussed in some detail. The anisotropic parameters such as dipolar couplings, that are at the root of the extreme complexity, can now be obtained reliably and can be used to derive detailed physical information about the solute. The direct dipolar couplings in particular can be interpreted in terms of solute geometry.

Since the ^{1}H NMR spectra of solutes dissolved in anisotropic media are usually superimposed on a strong undulating background arising from the liquid-crystal solvent, background removal is an important issue. When the number of transitions in the solute spectrum becomes very large, lines start to overlap. When much overlap is present, it becomes somewhat problematic to extract a typical experimental line width from the solute spectrum. In such a case the line width can be introduced as a fitting parameter in the evolutionary algorithm. Clearly, when the overlap increases further, it will get to the point where even our evolutionary strategies have difficulty in dealing with the line width problem, and extracting reliable values becomes an important issue.

The 2 examples discussed in this paper show the various aspects of how to apply evolutionary strategies and how to deal with the various peculiarities that may occur.

TABLE 2 Results of fits to the dipolar couplings as a function of temperature

	Line width/Hz		
Temperature/K	S_{zz}	W_{tcb}	$W_{exch} = W_{exp} - W_{tcb}$
302.8	−0.101	1.2	18.8
308.5	−0.096	1.8	15.2
314.2	−0.089	2.2	7.8
320.0	−0.083	4	8
325.6	−0.074	4	6
331.3	−0.059	6	2
332.4	−0.055	7	1

The dipolar couplings obtained for the 320.0 K spectrum (with J values fixed from ref 56) are $D_{12} = 937.5$ Hz, $D_{13} = -102.2$ Hz, $D_{14} = -40.8$ Hz, $D_{15} = -170.4$ Hz, $D_{16} = -49.3$ Hz, $D_{17} = -51.0$ Hz, and $D_{18} = -8.2$ Hz.

As illustrations we discuss 2 solutes that represent long-standing issues in organic chemistry. With the present techniques we are able to add significantly to the solution of these classical problems.

The first example is that of the solute hexamethylbenzene (C_6H_{18}). This 18-spin system shows more than 350 000 transitions and overlap of individual lines cannot be avoided. In this case our evolutionary strategy works well and the direct dipolar couplings are extracted. An analysis of these couplings shows that the internal rotation of the 6 methyl groups takes place in such a way as to avoid as much as possible steric hindrance between them. The intuitive notion that the methyl rotations in this molecule undergo a sixfold gearing motion is supported by our work.

The second example deals with a temperature study of the solute cyclohexane (C_6H_{12}), which is a textbook example of molecular interconversion between mirror-image chair conformations on the NMR time scale for motional averaging. Depending on temperature, this interconversion can be in the slow, intermediate or fast limit, with important consequences for the line width of each transition. This line width problem contributes to excessive spectral overlap of the 30 000 transitions with intensity >1% of maximum, thus inhibiting the extraction of reliable dipolar couplings. Using the line width as a fitting parameter in the evolutionary strategy in this case seems to lead to an overestimate. Fortunately, non-overlapping lines in the centre of the spectrum provide some guidance here. From the measured dipolar couplings, information about interconversion rates that agrees reasonably well with that from older experiments is obtained.

In summary, the use of evolutionary strategies in NMR has already been shown to be eminently feasible and will undoubtedly find many more novel applications. The successful application of the liquid-crystal method to a number of classical problems in organic chemistry is very encouraging. In this sense the use of liquid-crystal spectroscopy of solutes of larger size, leading to more extreme associated spectral complexity than ever before, has obtained a new lease of life.

ACKNOWLEDGMENTS

EEB is grateful to the Harrison Trust (UBC) for financial support.

ORCID

E. Elliott Burnell http://orcid.org/0000-0001-5569-5418

REFERENCES

1. Pople JA, Schneider WG, Bernstein HJ. *High-Resolution Nuclear Magnetic Resonance*. New York, NY: McGraw-Hill; 1959.
2. Corio PL. *Structure of High-Resolution NMR Spectra*. New York, NY: Academic Press; 1966.
3. Buckingham AD, McLauchlan KA. *Progress in Nuclear Magnetic Resonance Spectroscopy*, vol. 2. Oxford, UK: Pergamon Press; 1967:63.
4. Diehl P, Khetrapal CL. *NMR Basic Principles and Progress*, vol. 1. Berlin, Germany: Springer-Verlag; 1969:1.
5. Emsley JW, Lindon JC. *NMR Spectroscopy using Liquid Crystal Solvents*. Oxford, UK: Pergamon Press; 1975.
6. Burnell EE, de Lange CA. Prediction from molecular shape of solute orientational order in liquid crystals. *Chem Rev.* (Washington, D.C.), 1998;98:2359-2387.
7. Burnell EE, de Lange CA, eds. *NMR of Ordered Liquids*. Dordrecht, The Netherlands: Kluwer Academic Publishers; 2003.
8. Burnell EE, de Lange CA. ^{1}H and ^{2}H NMR of methanes partially oriented in liquid–crystal phases: separation of rigid and nonrigid molecule effects. *J Chem Phys.* 1982;76:3474-3479.
9. Burnell EE, de Lange CA, Barnhoorn JBS, Aben I, Levelt PF. Molecules with large-amplitude torsional motion partially oriented in a nematic liquid crystal: Ethane and isotopomers. *J Phys Chem A*. 2005;109:11027-11036.
10. Burnell EE, ter Beek LC, Sun Z. Mechanisms of solute orientational order in nematic liquid crystals. *J Chem Phys*. 2008;128:164901.
11. Weber ACJ, de Lange CA, Meerts WL, Burnell EE. The butane condensed matter conformational problem. *Chem Phys Lett*. 2010;496:257-262.
12. Burnell EE, Weber ACJ, de Lange CA, Meerts WL, Dong RYJ. Nuclear magnetic resonance study of alkane conformational statistics. *J Chem Phys*. 2011;135:234506.
13. Burnell EE, Weber ACJ, Dong RY, Meerts WL, de Lange CA. A model-free temperature-dependent conformational study of n-pentane in nematic liquid crystals. *J Chem Phys*. 2015;142:024904.
14. Weber ACJ, Burnell EE, Meerts WL, de Lange CA, Dong RY, Muccioli L, Pizzirusso A, Zannoni C. Communication: molecular dynamics and ^{1}H NMR of *n*-hexane in liquid crystals. *J Chem Phys*. 2015;143:011103.
15. Buckingham AD, Burnell EE, de Lange CA. Nuclear magnetic resonance spectra of hydrogen in a nematic phase. *Chem Comm*. 1968;1408-1409.
16. Burnell EE, de Lange CA, Snijders JG. Nuclear magnetic resonance study of H_2, HD, and D_2 in nematic solvents. *Phys Rev A*. 1982;25:2339-2350.
17. Burnell EE, de Lange CA, Segre AL, Capitani D, Angelini G, Lilla G, Barnhoorn JBS. Tritium nuclear magnetic resonance study of T_2, HT, and DT dissolved in nematic solvents. *Phys Rev E*. 1997;55:496-503.
18. Diehl P, Kellerhals H, Lustig E. *NMR Basic Principles and Progress*, Vol 6. Berlin, Germany: Springer-Verlag; 1972: 1.
19. Castellano S, Bothner-By AA. Analysis of NMR spectra by least squares. *J. Chem. Phys*. 1964;41:3863-3869.
20. Diehl P, Sýkora S, Vogt J. Automatic analysis of NMR spectra: an alternative approach. *J Magn Reson*. 1975;19:67-82.
21. Diehl P, Vogt J. Automatic analysis of n.m.r. spectra; a practical application to the spectra of oriented 2,4-dichlorobenzaldehyde and 2-chlorobenzaldehyde. *Org Magn Reson*, 1976;8:638-642.
22. Stephenson DS, Binsch G. Automated analysis of high-resolution NMR spectra. I. Principles and computational strategy. *J Magn Reson*. 1980;37:395-407.

23. Stephenson DS, Binsch G. Automated analysis of high-resolution NMR spectra. II. Illustrative applications of the computer program DAVINS. *J Magn Reson*. 1980;37:409-430.
24. Stephenson DS, Binsch G. Automated analysis of high-resolution NMR spectra III—the nematic phase spectra of three allyl halides. *Org Magn Reson*. 1980;14:226-233.
25. Stephenson DS, Binsch G. The molecular structure of cyclopentene in solution as obtained from a nematic phase proton N.M.R. study. *Mol Phys*. 1981;43:697-710.
26. Stephenson DS. Encyclopedia of magnetic resonance. Analysis of spectra: automatic methods. *eMagRes*. 2007; https://doi.org/10.1002/9780470034590.emrstm0013
27. Castiglione F, Carravetta M, Celebre G, Longeri M. Toward a generalized algorithm for the automated analysis of complex anisotropic NMR spectra. *J Magn Reson*, 1998;132:1-12.
28. Castiglione F, Celebre G, De Luca G, Longeri M. The NMR spectra of samples dissolved in liquid–crystalline phases: automatic analysis with the aid of multiple quantum spectra— the case of flexible molecules. *J Magn Reson*. 2000;142:216-228.
29. Longeri M, Celebre G. Encyclopedia of magnetic resonance. Liquid crystalline samples: spectral analysis. *eMagRes*. 2007; https://doi.org/10.1002/9780470034590.emrstm0268
30. Takeuchi H, Inoue K, Ando Y, Konaka S. Efficient method to analyze NMR spectra of solutes in liquid crystals: the use of genetic algorithm and integral curves. *Chem Lett*. 2000;29:1300-1301.
31. Inoue K, Takeuchi H, Konaka S. Molecular structures of related compounds of mesogens studied by ^{1}H NMR using a liquid crystal solvent: tolan and *trans*-azobenzene. *J Phys Chem A*, 2001;105:6711-6716.
32. Meerts WL, Schmitt M. Application of genetic algorithms in automated assignments of high-resolution spectra. *Int Rev Phys Chem*. 2006;25:353-406.
33. Meerts WL, de Lange CA, Weber ACJ, Burnell EE. *Encyclopedia of Magnetic Resonance, Analysis of Complex High-resolution NMR Spectra by Sophisticated Evolutionary Strategies*. *eMagRes*. 2013;437-450. https://doi.org/10.1002/9780470034590.emrstm1309
34. Burnell EE, de Lange CA, Meerts WL. Communication: molecular gears. *J Chem Phys*. 2016;145:091101.
35. Burnell EE, de Lange CA. On the average orientation of molecules undergoing large-amplitude conformational changes in anisotropic liquids. *Chem Phys Lett*. 1980;76:268-272.
36. de Lange CA, Meerts WL, Weber ACJ, Burnell EE. Scope and limitations of accurate structure determination of solutes dissolved in liquid crystals. *J Phys Chem A*. 2010;114:5878-5887.
37. Holland JH. *Adaption in Natural and Artificial Systems*. Ann-Arbor, MI: The University of Michigan Press; 1975.
38. Rechenberg I. *Evolutionsstrategie - Optimierung technischer Systeme nach Prinzipien der biologischen Evolution*. Stuttgart, Germany: Frommann-Holzboog; 1973.
39. Schwevel H-P. *Evolution and Optimum Seeking*. New York, NY: John Wiley & Son; 1993.
40. Hansen N, Ostermeier A. Completely derandomized self-adaptation in evolution strategies. *Evol Comput*. 2001;9:159-195.
41. Ostermeier A, Gawelczyk A, Hansen N. Step-size adaptation based on non-local use of selection Information. In: *Lecture notes in Computer Science: Parallel Problem Solving from Nature (PPSN III)*. Berlin, Germany: Springer; 1994: 189-198.
42. Hansen N, Kern S. Evaluating the CMA evolution strategy on multimodal test functions. In: Yao X, et al., eds. *Parallel Problem Solving from Nature PPSN VIII, Volume 3242 of LNCS*. Berlin/Heidelberg, Germany: Springer; 2004:282-291.
43. Altay A, Kayakutlu G, Topcu YI. Win–win match using a genetic algorithm. *Appl Math Mod*, 2010;34:2749-2762.
44. Garuti C, Salomon VAP. Compatibility indices between priority vectors. *Int J Analyt Hierarchy Proc*. 2012;4:152-160.
45. Saaty TL. A ratio scale metric and the compatibility of ratio scales: the possibility of arrow's impossibility theorem. *Appl Math Lett*. 1994;7:51-57.
46. Pearson K. Note on regression and inheritance in the case of two parents. *Proc Royal Soc Lond*. 1895;58:240-242.
47. Meerts WL, Schmitt M, Groenenboom GC. New applications of the genetic algorithm for the interpretation of high-resolution spectra. *Can J Chem*. 2004;82:804-819.
48. Hageman JA, Wehrens R, de Gelder R, Meerts WL, Buydens LMC. Direct determination of molecular constants from rovibronic spectra with genetic algorithms. *J Chem Phys*. 2000;113:7955-7962.
49. Iroff LD. On the gearing of methyl groups in hexamethylbenzene. *J Computational Chem*. 1980;1:76-80.
50. Melissas V, Faegri Jr. K, Almloef J. Rotation of methyl groups in hexamethylbenzene. *J Am Chem Soc*. 1985;107:4640-4642.
51. Gaussian 09, Revision D.01, Frisch MJ, et al. Wallingford, CT: Gaussian, Inc.; 2013.
52. Møller C, Plesset MS. Note on an approximation treatment for many-electron systems. *Phys Rev*. 1934;46:618-622.
53. Dunning TH. Gaussian basis sets for use in correlated molecular calculations. I. The atoms boron through neon and hydrogen. *J Chem Phys*. 1989;90:1007-1023.
54. Luz Z. Chapter 19. In: Burnell EE, de Lange CA, eds. *NMR of Ordered Liquids*. Dordrecht, The Netherlands: Kluwer Academic Publishers; 2003.
55. McConnell HM. Reaction rates by nuclear magnetic resonance. *J Chem Phys*. 1958;28:430-431.
56. Garbisch EW Jr., Griffith MG. Proton couplings in cyclohexane. *J Am Chem Soc*. 1968;90:6543-6544.
57. Pickett HM, Strauss HL. Conformational structure, energy, and inversion rates of cyclohexane and some related oxanes. *J Am Chem Soc*. 1970;92:7281-7290.
58. Bain AD, Baron M, Burger SK, Kowalewski VJ, Rodriguez MB. Interconversion Study in 1,4-substituted six-membered cyclohexane-type rings. Structure and dynamics of *trans*-1,4-Dibromo-1,4-dicyanocyclohexane. *J Phys Chem A*. 2011;115:9207-9216.

How to cite this article: Burnell EE, de Lange CA, Dong RY, Meerts WL, Weber ACJ. Evolutionary algorithms and nuclear magnetic resonance of oriented molecules. *Concepts Magn Reson Part A*. 2016;45A: e21415. https://doi.org/10.1002/cmr.a.21415